Outage Prediction during Intense Rainstorm Events Using Queuing Theory and Markov Chains over Radio Links

Mary N. Ahuna[1], *, Thomas J. Afullo[1], and Akintunde A. Alonge[2]

Abstract—Satellite communication links operating at higher frequency bands suffer from signal outages due to rain attenuation. Site diversity technique is one of the rain fade mitigation techniques that can be employed over earth-satellite links to improve on system availability. In this study, we use 5-year rainfall rate statistics and the queuing theory approach to investigate the attributes and behavior of intense rain storms along an earth-space link over Durban, South Africa ($29° 52$'S, $30° 58$'E), a sub-tropical climate. Thereafter, a comparison is made with results obtained in a related study in Jimma, Ethiopia ($7.6667° $N, $36.8333° $E), which is a tropical climatic region. Verification of the best fit distribution is done through the application of the root mean square error (RMSE) and CHI squared statistics. Results of these analysis tools confirm the suitability of the proposed distributions with RMSE error margin in the range 0.0024 to 0.0128, and a χ^2 statistics value of 0.4070. The spike service time for such rain storms is found to follow Erlang-k distribution in both regions of South Africa and Ethiopia as opposed to earlier determined exponential distribution. In addition, the analysis shows that there exists a power law relationship between the rain spike maximum rain rate and its diameter. This relationship is further utilized in the development of the rain cell sizing model that can be used for site diversity fade mitigation. Furthermore, the Markov chain technique is employed to determine the occurrence behavior of shower and storm rainfall regimes, and their contributions to rain attenuation over a slant path radio link.

1. INTRODUCTION

Wireless communication over frequency bands above 10 GHz brings along the much needed bandwidths for fast and efficient communication via satellite and terrestrial communication links [1]. The current tasks of 5G technologies entails benefits of faster speeds, higher bandwidths and lower latency. For these benefits to suffice, wireless links need to experience close to zero link outages. However, in the presence of heavy rain storms, wireless microwave links operating at 5 GHz and above cannot be guaranteed to provide such high efficiency service due to signal fading that results from wave absorption and scattering by rain drops [2–4]; this eventually leads to signal attenuation. Strategies have to be implemented to ensure that even in the presence of storms, the wireless link is at least available for 99.99% of the time or better. Designers of radio links operating in Ku-bands and beyond are thus rightly concerned about link availability even during a natural phenomenon like a rainfall event.

Accurate prediction of a rain storm and the corresponding magnitude of signal attenuation plays a crucial role in mitigating link fades and outages. Predicting the duration and rate of occurrence of these fades is also important to the link design engineer for deployment of counter-measures that will eventually guarantee high link availabilities.

Due to the rising of storms over the location of study, this paper explores the probability of occurrence of storms of different magnitudes for efficient planning and mitigation of link outages due to the rain occurrence. This paper is structured thus: Section 2 gives a brief summary of related work that has been done on queueing theory approach to rain modelling, while Section 3, introduces the model of a rain storm using a unified model language (UML) representation. Section 4 highlights the data measurement campaign and processing, whereas Section 5 presents storm occurrence trends over Durban. Results are presented and discussed in Section 6. Section 7 provides the conclusion of the study.

2. RELATED WORK

The queuing theory concept develops information on the behavior of queuing systems, paving way for informed decisions during problem-solving campaigns. Three main random variables used with queueing theory problems being the inter-arrival time, the service time and the overlap time [5–8]. *Alonge and Afullo* [7] pioneered research work in the use of queuing theory for rainfall modelling over Durban, a subtropical climatic region. Using this approach, they proposed a non-Markovian distribution for rainfall service time, t_{st}, as [7]:

$$f\left(t_{st}\right) = \frac{k\mu(k\mu t_{st})^{k-1}e^{-k\mu t_{st}}}{\Gamma(k)} \quad \text{for} \ \ t_{st} > 0 \tag{1}$$

where μ is the data service rate, and k is the Erlang-k number of stages. For the inter-arrival time distribution, they proposed the exponential distribution that follows a Markovian process, given by:

$$f\left(t_{arr}\right) = \lambda e^{-\lambda t_{arr}} \quad \text{for} \ \ t_{arr} > 0 \tag{2}$$

where t_{arr} is the inter-arrival time and λ is the data arrival rate.

Resulting from their studies, *Alonge and Afullo* [9] concluded that the steady state queue discipline follows a semi-Markovian first come first served (FCFS), M/E_R queue discipline, for tropical and subtropical locations.

In 2016, *Diba et al.* [10] applied the same approach to the study of rainfall synthesis in Jimma, Ethiopia. Furthermore, they characterized rainfall rate spikes over Jimma using Markov chain and queuing models. The results of their study showed that rain spike service time follows the Erlang-k probability distribution contrary to the common exponential distribution.

Figure 1 shows four attributes of a rain event, which were analyzed in this study. These attributes are rain spike service time, (t_{st}); spike inter-arrival time (t_{arr}); spike overlap time (t_{ov}); and maximum spike rainfall rate (R_m).
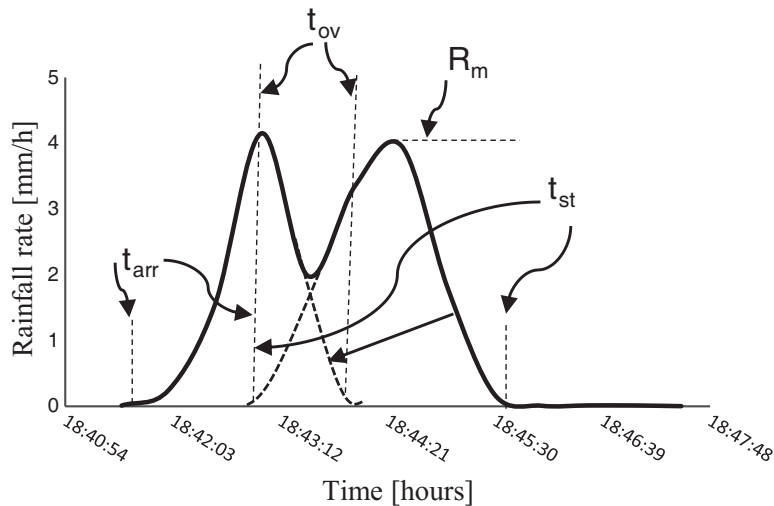

Figure 1. A rainfall drizzle event of 16th August, 2016 at 18:41:30 hours.
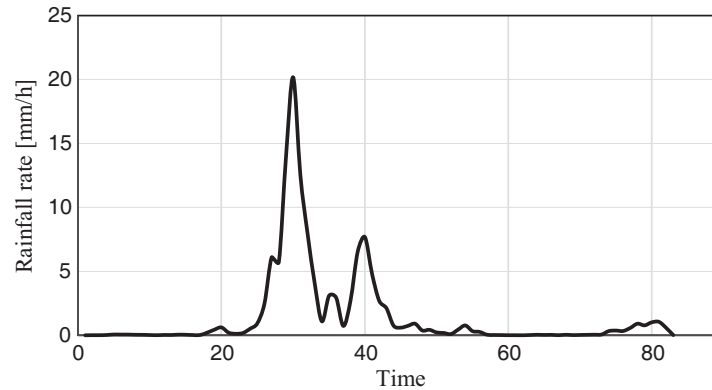
Figure 2. A rainfall shower event of 8th January, 2017 at 09:04:00 hours.

A typical rain event comprises rainfall spikes of varying heights and width over time as shown in Figure 2. This variability of occurrence of rain spikes with varying magnitudes and width makes it hard to predict the height or width of the next rain spike. At the onset of a rain event, a single rain spike progressively builds up from near zero to a spike maximum rate, then the magnitudes start reducing with time [9]. This is analogous to a birth-death process. From the queueing theory concept, a spike is related to a single cloud with a maximum intensity at its center. Consequently, we visualize rain spikes, similar to those displayed in Figure 2, as formed by a queue of clouds passing over a rain measurement instrument one after the other in a first come first served (FCFS) discipline.

Begum and Otung [11] applied synthetic storm technique and rain rate time series to determine the partial structure of the rain cells over Sparsholt, UK. Their results show that intense rain cells have generally less than 10 km. In 2011, *Akuon and Afullo* [12] investigated rain cell sizes over different climatic regions within South Africa using synthetic storm technique and derived 1-minute rainfall distributions. Their results show that distances of up to 7.75 km are realized for rain rate threshold of 60 mm/h.

3. RAIN STORM MODELLING USING THE UNIFIED MODEL LANGUAGE CONCEPT

Relationships existing between elements of a rain storm can be modelled using the Unified Model Language (UML) concept [13]. In this modelling, *class diagrams* are used to show how entities are modelled within a system. A *class* represents an abstraction of an entity with common characteristics whereas *associations* represent relationships between classes. Aside from describing the *attributes* and *operations* of a class, the class diagram also shows *constraints* imposed on a class.

Using the class diagram model in Figure 3, we extended this model to a thunderstorm rain event as illustrated in Figure 4. A rain storm entity is modelled as a UML class diagram, as shown in Figure 4, with associations between the rain storm, storms and spikes. For instance, in Figure 4, the cardinality of the rain spike in the storm-spike association is, given as '2...*' implying that a storm can be made up of 2 or more rain spikes. This constraint ensures that the three required rain spike attributes (queueing parameters) namely service time, inter-arrival time and overlap time, can be extracted from the storm event. At the storm end, the cardinality is given as '1...1', which means that a particular rain spike can only belong to one and only one rain storm type. If, by chance, two spikes have similar rainfall rates, deeper analysis will reveal that their drop size distributions will differ, hence their impact on the signal will be different. Operations for the storm class are *start* and *end*, implying that every storm is characterized by the starting and ending operations/actions. Similarly, the operations for the rain spike are given as *birth* and *death*. This birth-death (BD) behavior of a typical rain spike was highlighted in *Alonge and afullo* [9], where the death process starts after the spike has attained its maximum rain rate, R_m. In Figure 4, all three classes are responsible for causing signal attenuation. This attenuation could be harmless, like that caused by drizzle and widespread spikes, or severe, when caused by rain spikes with very high magnitudes in Storm 2 and Storm 3 rain events (*see clarification in Table 1*).
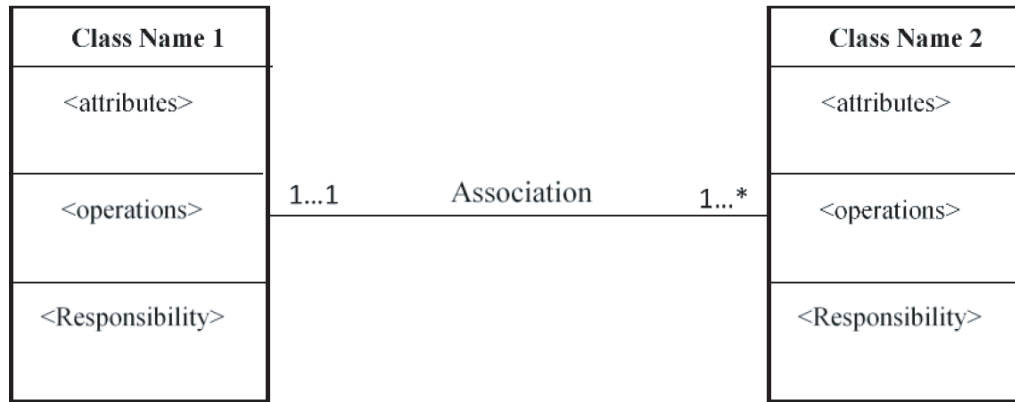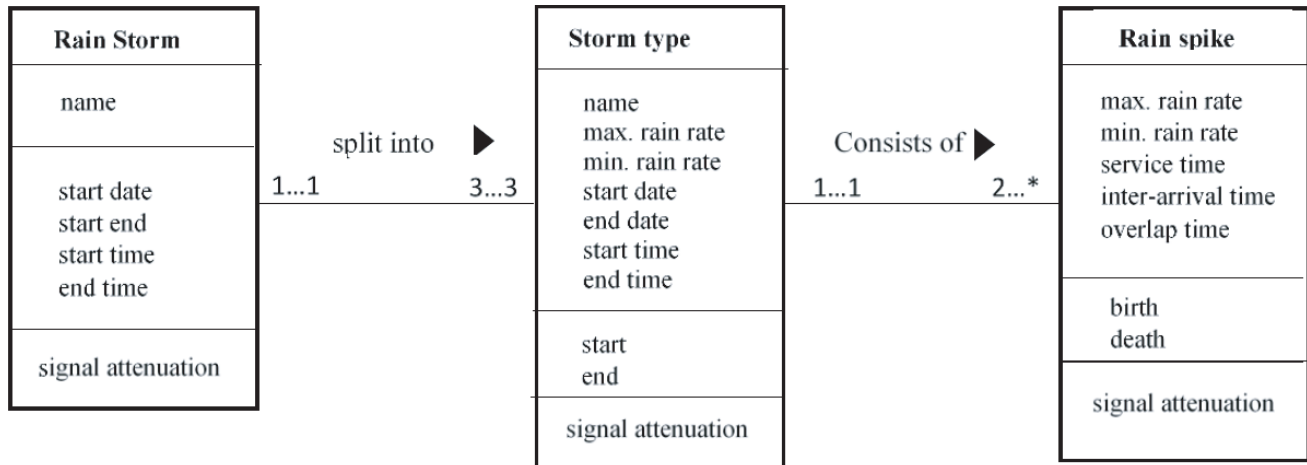
Figure 3. A typical class diagram.

Figure 4. Rain storm entity class diagram.

Table 1. Data extracted from shower and storms regimes.

Rain Rate Regime	Max Peak Rain Rate [mm/h]	Samples used	%
Drizzle (D)	$R < 5$	125	17.6
Widespread (W)	$5 \leq R < 10$	130	18.3
Shower (Sh)	$10 \leq R < 40$	283	39.8
Storm 1 (S_1)	$40 \leq R \leq 100$	135	19.0
Storm 2 (S_2)	$100 < R \leq 150$	20	2.8
Storm 3 (S_3)	$R > 150$	18	2.5

4. DATA COLLECTION AND PROCESSING

The data used in this study was measured by the Joss-Waldvögel (JW) RD-80 disdrometer instrument installed on the rooftop of the Electrical North Building, Howard Campus, University of KwaZulu Natal, Durban, South Africa. This instrument comprises of an outdoor unit with rain drops capturing surface area measuring $0.005\,\text{m}^2$, and an indoor unit comprising of a processor and a computer. Data sampling/integration time is 30 seconds. For full description and set-up, see [14, 15]. Data used in this

study was retrieved from convective type of rain events in the shower and thunderstorms regimes due to their higher contribution to signal attenuation over LOS radio communication links.

In this study, rainstorms over Durban are further subdivided into three groups following a sudden experience of heavy rain storms in the years 2016 and 2017. This sudden turnaround of events generated a considerable gap between the minimum and the maximum rainfall rates within the thunderstorm regime. From previous measurements, the gap used to be about 40 mm/h in the years 2015 and earlier. But then, right from the onset of the year 2016, this gap rose to over 200 mm/h and the same large gap was still seen in 2017. Accordingly, data used in this work is categorized into the following regimes: Drizzle (D), Widespread (W), Shower (Sh), Storm 1 (S_1), Storm 2 (S_2) and Storm 3 (S_3). For clarity, the inclusion of drizzle and widespread rain spikes in our categories arises because a typical thunderstorm rain event builds up starting from drizzle rainfall rates and progressively into widespread rain rate range before moving into shower thunderstorm regime rain rates as shown in Figure 1 and Figure 2.

5. STORM OCCURRENCE PATTERN OVER DURBAN

Precipitation analysis of storm occurrence over Durban is done for a period of 57 consecutive months (4.75 years) spanning from April 2013 to December 2017. This analysis is based on shower and storm regimes with a rainfall rate $10 \leq R < 40$ mm/h and $R \geq 40$ mm/h respectively. This is motivated by the immense contribution of these higher rainfall rates in radio link outages during a rainfall event. Further subdivision of these storms are as given in Table 1.

As observed in Figure 5 and Table 2, there were more rain storms in 2016 than other four years. Nonetheless, in 2017, despite experiencing half the number of storms compared to the year 2016, it
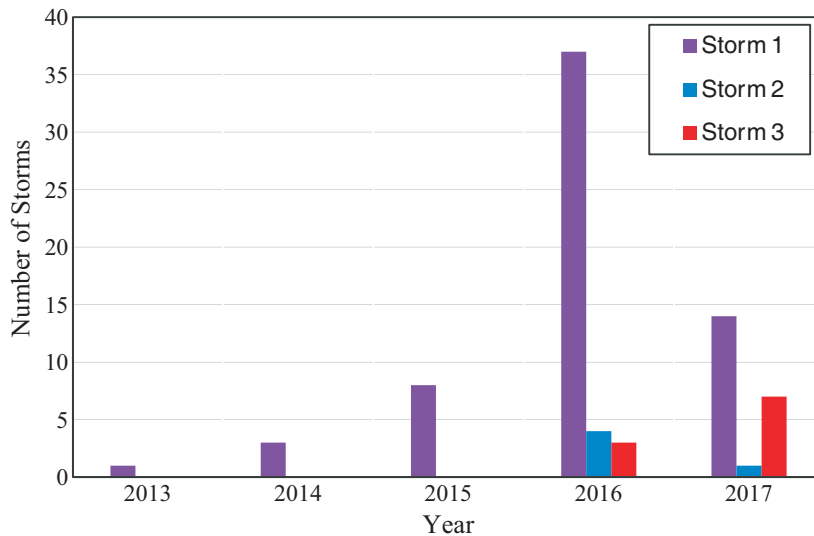

Figure 5. Storm occurrence pattern over Durban.

Table 2. Storm occurrence over Durban, South Africa.

Storm Type	Number of storm occurrences					
	2013	2014	2015	2016	2017	Total
S_1	1	3	8	37	14	63
S_2	0	0	0	4	1	5
S_3	0	0	0	3	7	10
Total	1	3	8	44	22	**78**
Storm days	1	3	7	30	16	

experienced more S_2 storms, almost double the number experienced in 2016. From Table 2, it is noticed that 58.73% of S_1 storms were experienced in 2016, and neither S_2 nor S_3 storms ever occurred in the previous three years of 2013, 2014 and 2015.

6. ANALYSIS OF SHOWER AND STORM EVENTS

As mentioned earlier in Section 2, basic queuing parameters of interest in this study are spike service time, spike inter-arrival time and spike overlap time. These parameters are extracted from rainfall spikes constituted in shower and storm rain events and the results are summarized in Table 3. Thereafter, probabilities of occurrence of varying magnitudes of these spikes and their contributions to link attenuation are analyzed.

Table 3. Spike queuing parameters for shower and storm regimes.

	Rainfall regime	Average time [mins]	Best fit Distribution	RMSE	CHI
Service time,	$c_{x,Sh} = 0.7201$	21.13	Erlang-k, $k = 2$	0.0059	0.0931
t_{st},	$c_{x,St} = 0.6712$	13.00	Erlang-k, $k = 3$	0.0092	0.2390
Inter-arrival Time,	$c_{x,Sh} = 0.4807$	16.28	Erlang-k, $k = 2$	0.0057	0. 2306
t_{arr}	$c_{x,St} = 1.0996$	8.47	Exponential	0.0092	0.1445
Overlap Time,	$c_{x,Sh} = 0.8702$	3.16	Erlang-k, $k = 2$	0.0128	0.4070
t_{ov}	$c_{x,St} = 0.6067$	2.79	Erlang-k, $k = 3$	0.0471	0.1563
Spike Max. Rain Rate,	$c_{x,Sh} = 0.7335$	-	Erlang-k, $k = 2$	0.0068	0.0352
R_m	$c_{x,St} = 0.8964$	-	Exponential	0.0024	0.0609

$c_{x,Sh}$ and $c_{x,st}$ are coefficients of variation for shower and storms regimes respectively

6.1. Spike Service Time Distributions

Figure 6 shows distribution fittings of the queue parameters generated. It is observed that rain spike service time and spike overlap time for both shower and storm events follow the Erlang-k distribution with $k = 2$ as the number of stages for shower regimes and $k = 3$ for storms over 40 mm/h rainfall rate. The Erlang-k distribution is given by [7, 16]:

$$f(x) = \mu \frac{(\mu x)^{k-1}}{(k-1)!} e^{-\mu x} \tag{3}$$

where μ is the scale parameter and k is the shape parameter.

Figure 7 shows the number of rain spikes for which spike service time is exceeded. It is observed that for the same spike service time, there are more than twice the number of shower spikes as there are storm spikes. This indicates that the duration a spike takes to traverse a given area decreases as the spike magnitude increases. For instance, in Table 3, it is shown that it takes an average of 21.13 minutes for a shower spike to traverse a given region. On the other hand, a storm spike will take only 13.00 minutes for its traversal. This traversal time of 13.00 minutes is comparable to 13.32 minutes obtained by Diba et al. [10] for storms spikes over Jimma, Ethiopia, as shown in Table 4. Results of this table relates this current work with the previous work carried out by Diba et al. [10] over Jimma, Ethiopia. From Table 4, analysis shows that average service times for shower spikes are 21.1336 minutes and 16.8390 minutes for Durban and Jimma respectively. This shows that a shower spike over Durban takes approximately 4.2946 minutes longer to traverse an observation point than its counterpart over Jimma. For rain storm events, spike average service time is comparatively very close to values of 13.0028 minutes and 13.3237 minutes for Durban and Jimma respectively. Further analysis shows that service time distributions at both sites can best be represented by Erlang-k distribution with the value of k in
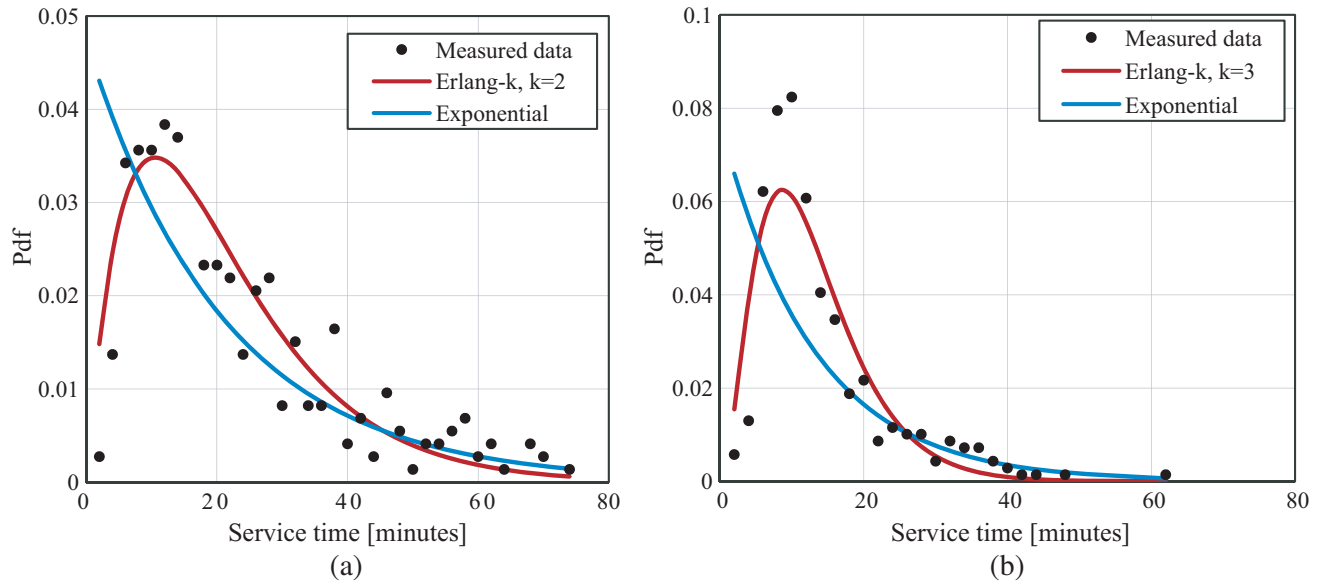
Figure 6. Service time distributions for (a) shower and (b) storm rainfall regimes.
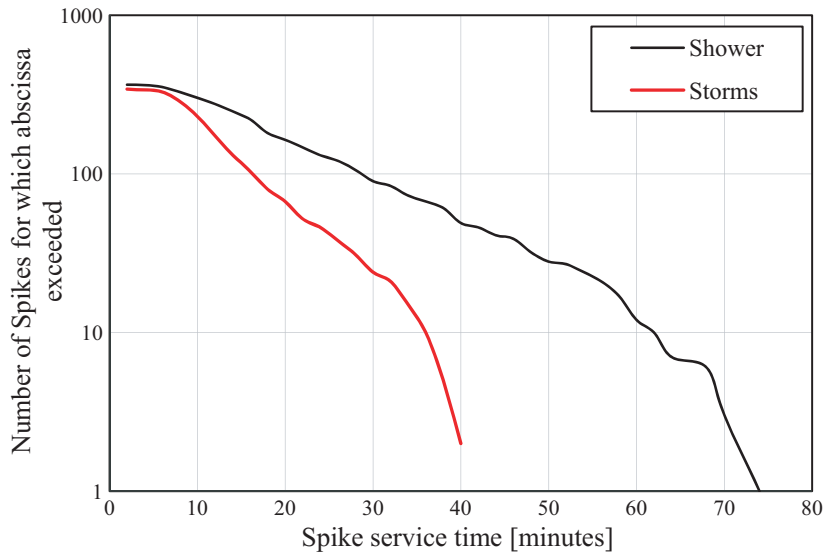

Figure 7. Rain spike duration exceedance [minutes].

the range $2 \leq k \leq 4$. Also, coefficients of variation (CV) values are shown to be higher for rain storms than shower storms. (*See Table 4*).

6.2. Spike Inter-Arrival Time Distributions

The inter-arrival time denotes arrival times of spikes over the point of observation. Inter-arrival times are presented in Table 3 for shower and storms regimes, and the results show that for spikes in shower regimes, the average inter-arrival time is 16.28 minutes, while for storms regimes, the average inter-arrival time is 8.47 minutes. Inter-arrival distributions are shown in Figure 8, and it is observed that while the inter-arrival time for the shower regime follows the Erlang-k distribution, with $k = 2$, the inter-arrival time distribution for storms with maximum rainfall rates greater than $40 \, \text{mm/h}$ follows the exponential distribution similar to results by *Alonge and Afullo* [7].

Table 4. Rain spike service time comparisons between Durban and Jimma.

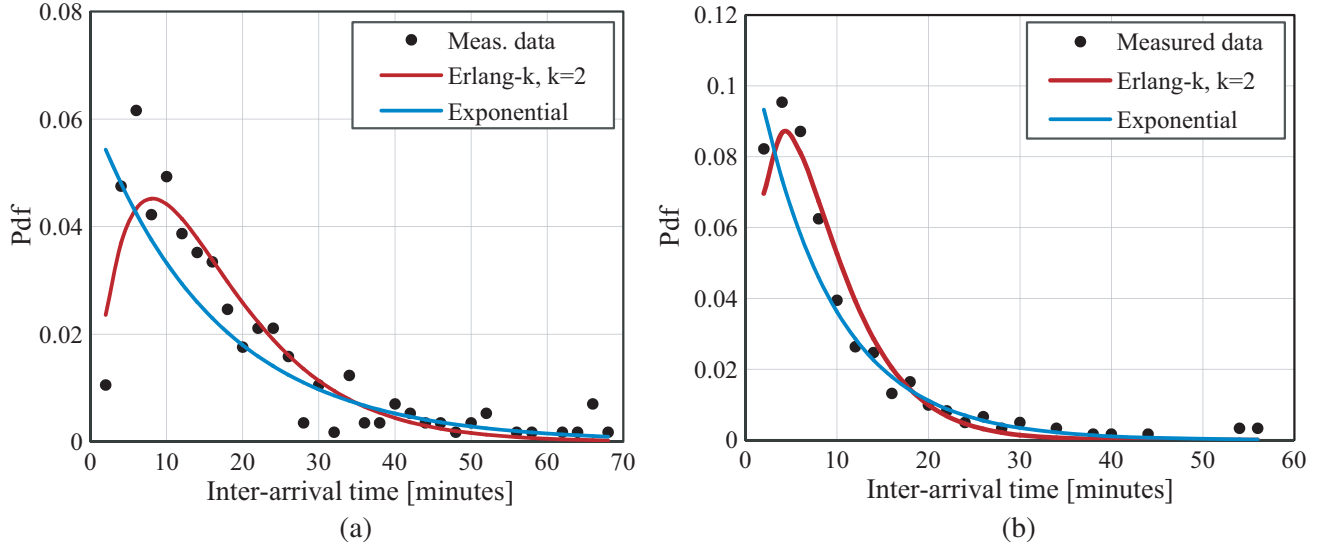| Model	Regime	Service time distribution	Average Spike Service Time (minutes)	CV
Diba et al. [8]	Shower	E_k, $k = 4$	16.8390	0.5357
(Jimma)	Storms	E_k, $k = 4$	13.3237	0.5862
Durban	Shower	E_k, $k = 2$	21.1336	0.4807
	Storms	E_k, $k = 3$	13.0028	1.0486

Figure 8. Inter-arrival time distributions for (a) shower and (b) rain storm regimes.

6.3. Spike Over-Lap Time Distributions

Rain spike cells are seen to overlap one another as shown in Figure 1 with a time, t_{ov}. This means that in a typical rainfall event, before a cell has exited, another cell appears, hence the formation of the overlap time. Table 3 shows that rain spikes in the shower events overlap with an average time of 3.16 minutes, while those in storms overlap with an average of 2.79 minutes. Results by *Alonge and Afullo* [7] showed a corresponding overlap time of 5.75 minutes for storms regime, over Durban. Their higher results for overlap time can be explained thus: their experimental data did not comprise of extreme storms (Storm 2 and Storm 3 types) referred to in this paper. It is to be noted that Storm 2 and Storm 3 types of rainfall regimes only emerged in year 2016 as shown in Figure 5. In support of this lower overlap time, higher magnitude storm spikes tend to rise and fall faster hence reduced overlap time. In addition, from *Section 6.4*, it is shown that service time decreases with increase in maximum spike rain rate.

Figure 9 shows fitting distributions for the overlap time distributions for both shower and storm regimes. It is seen that these distributions follow the Erlang-k distribution with $k = 2$ and $k = 3$ for shower and storm, respectively, similar to their service times counterparts. These results are expected because the overlap time parameter is a subset of the spike service time.

6.4. Correlation between Spike Maximum Rain Rate with Spike Diameter

Distributions of spike maximum rain rate are presented in Figure 10. It is observed that shower regimes can be modeled by Erlang-k distribution whereas the storm events can be modelled using the exponential distribution. Analysis of service time queuing parameters together with advection velocities of 6 m/s and
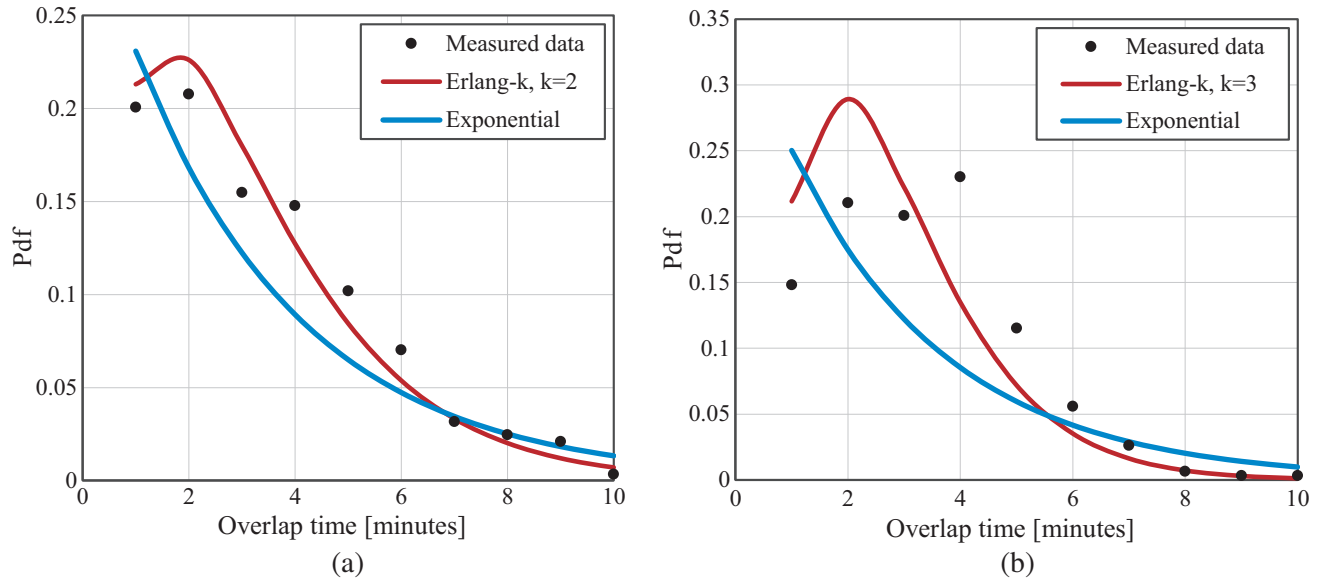
Figure 9. Overlap time distributions for (a) shower and (b) storm rainfall regimes.
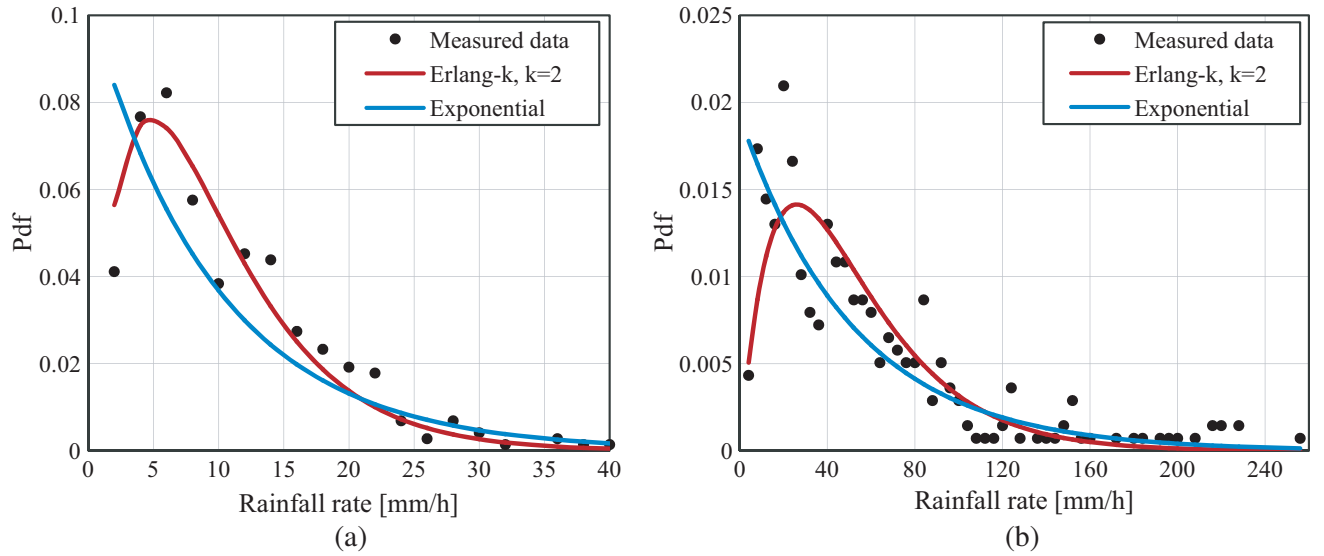

Figure 10. Spike maximum rainfall rate distributions for (a) shower and (b) thunderstorm rainfall regimes.

10 m/s for shower and storm events respectively were used to determine rain spike cell diameters [17, 18].

Relationships between spike diameters and spike maximum rainfall rates are shown in Figure 11; it is apparent that the diameter of a storm spike is a function of the maximum rain rate within a rain event. It is also observed that spikes with lower maximum rain rates have larger diameters than those spikes with high rainfall rates. For instance, spikes with maximum rain rates below 10 mm/h have averaged diameters of about 8.5 km. On the hand, rain spikes with maximum rain rates between 90–100 mm/h range have an average cell diameter of 4.8 km.

From Figure 11 it is observed that the rain cell spike maximum rainfall rate, R_m, and the spike diameter, D_{sp}, are related by the expression:

$$D_{sp} = c_1 R_m^{c_2} \text{ [km]} \tag{4}$$

where R_m is the maximum spike rain rate in mm/h, and coefficients c_1 and c_2 are given as 12.842 and
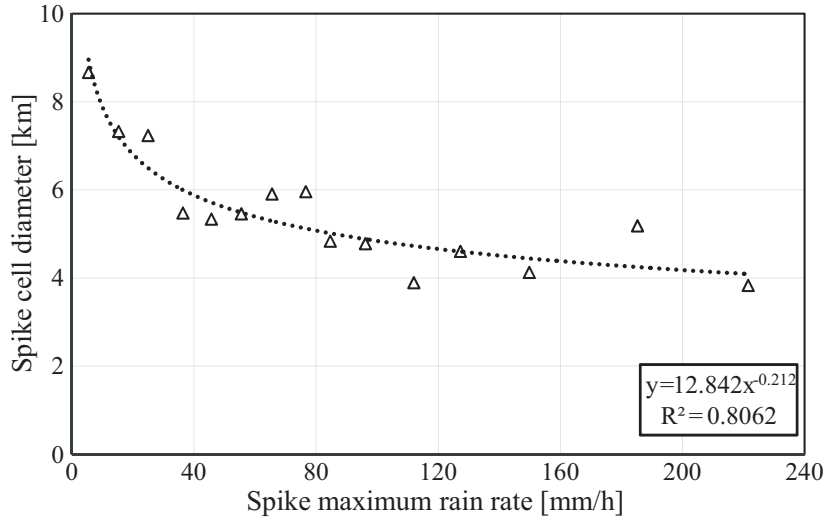
Figure 11. Spike diameter versus maximum spike rain rate for shower and storm rain events.

-0.212 respectively for Durban climatic region.

From the analysis of obtained queuing parameters, a rain event cell diameter, D_{ev}, can be approximated as:

$$D_{ev} \approx 4D_{sp} - 3D_{ov} \text{ [km]} \tag{5}$$

where D_{ov} is the overlap distance for two consecutive rain spikes, and D_{sp} is the rain spike diameter.

Analysis of rain events in this study showed that, on average, there are four rain spikes within a rain event for both shower and storms regimes. Therefore, from Eqs. (4), (5) and *Section 6.3*, distance coverage for any rain event can be determined. For example, for maximization of site diversity gain, the minimum distance, $D_{ev,\min}$, between stations is approximated to be 22 km, calculated from the minimum rain rate in the shower regime. For higher rainfall rates, cell diameters are less than $D_{ev,\min}$, hence any two stations will not fall under the same rain event of intense rainfall.

6.5. Model Validation

Data and statistical distribution fitting was carried out using the root mean square error (RMSE) and CHI squared (χ^2) tools represented by Eqs. (6) and (7) respectively for different statistical distributions with measured data. The two error fitting techniques are given by:

$$\text{RMSE} = \sqrt{\frac{1}{L} \sum_{i=1}^{L} \delta^2} \tag{6}$$

$$\chi^2 = \sum \frac{1}{O_i} (E_i - O_i)^2 \tag{7}$$

where δ is the error, L the number of samples, and E_i and O_i are the expected and actual outputs respectively. Error values obtained from Eqs. (6) and (7) are satisfactory. For instance, the highest values of 0.0128 and 0.4070 corresponding to RMSE and CHI squared statistics were obtained for the overlap time in the shower regime. A significance level of 5% was chosen for χ^2 statistics. With the critical value of 18.305 and degree of freedom of 10, the chosen model (Erlang-k, with $k = 2$) for spike overlap time ($\chi^2 = 0.4070$) is acceptable. This satisfaction criterion will apply to all other models chosen for other parameters because they have higher values of df and lower values of χ^2 values. Hence, all models chosen are acceptable, indicating that 95% of model values satisfy measured values.

6.6. Rain Spike Magnitude Prediction Using Markov Chain Approach

The knowledge of the probability of an incoming rain spike magnitude is important. This aids in predicting anticipated rain attenuation and therefore putting forth the right fade mitigation tools to ensure that the link fade does not fall below a given threshold. In this study, we have used the N-state Markov chains approach to investigate the behavior of measured rain storm patterns over the location of study for prediction of the magnitude of an incoming rain spike [19]. In this investigation, the number of states, N, is 6, where 'state' represents a rain regime type. These six states are: drizzle (D), widespread (W), shower (Sh), storm 1 (S_1), storm 2 (S_2) and storm 3 (S_3). This analysis was done using data in the shower and thunderstorm regimes due to their high contribution to signal attenuation. The state transition matrix for shower regime is a 3×3 matrix as shown in (8):

$$P_{ij,(shower)} = \begin{bmatrix} DD & DW & DSh \\ WD & WW & WSh \\ ShD & ShW & ShSh \end{bmatrix} \tag{8}$$

where DD is the state jump from one drizzle spike to another drizzle spike, WD is the state jump from widespread spike to drizzle spike and so on. From measured data, the rain spike transition graph for spikes in the shower regime are given in Figure 12, whereas the state transition matrix is given in (9):

$$P_{ij,(shower)} = \begin{bmatrix} 0.4609 & 0.2783 & 0.2609 \\ 0.2800 & 0.2000 & 0.5200 \\ 0.2483 & 0.3221 & 0.4295 \end{bmatrix} \tag{9}$$
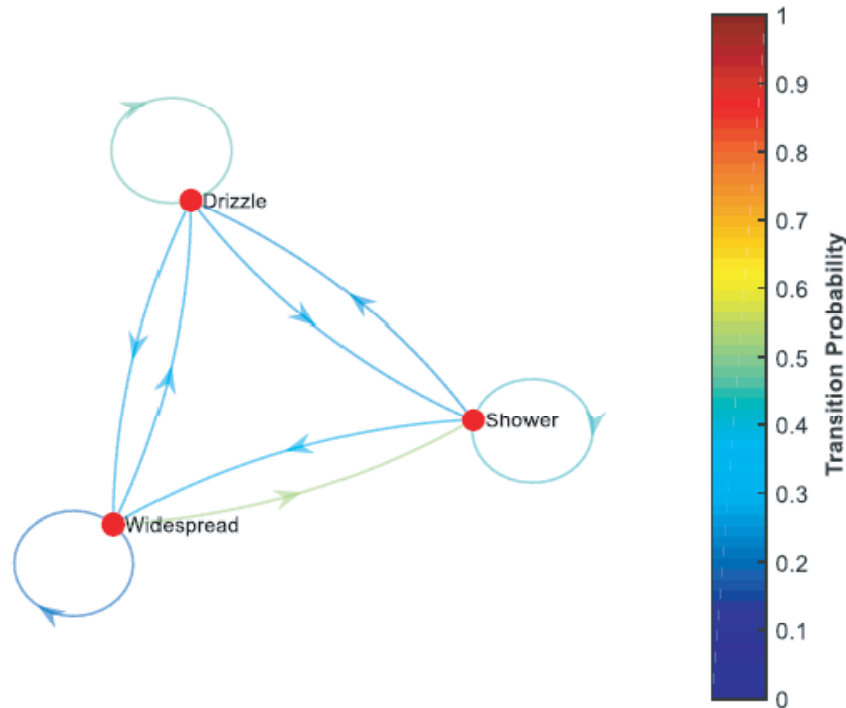

Figure 12. Spike transition graph for shower regime.

The initial probability matrix in Eq. (9) indicates that the highest number of state transitions occurs during transitions from widespread state to shower state, with a probability of 52%. The least probability of 20% is observed between two widespread states. For rain storm events, the transition
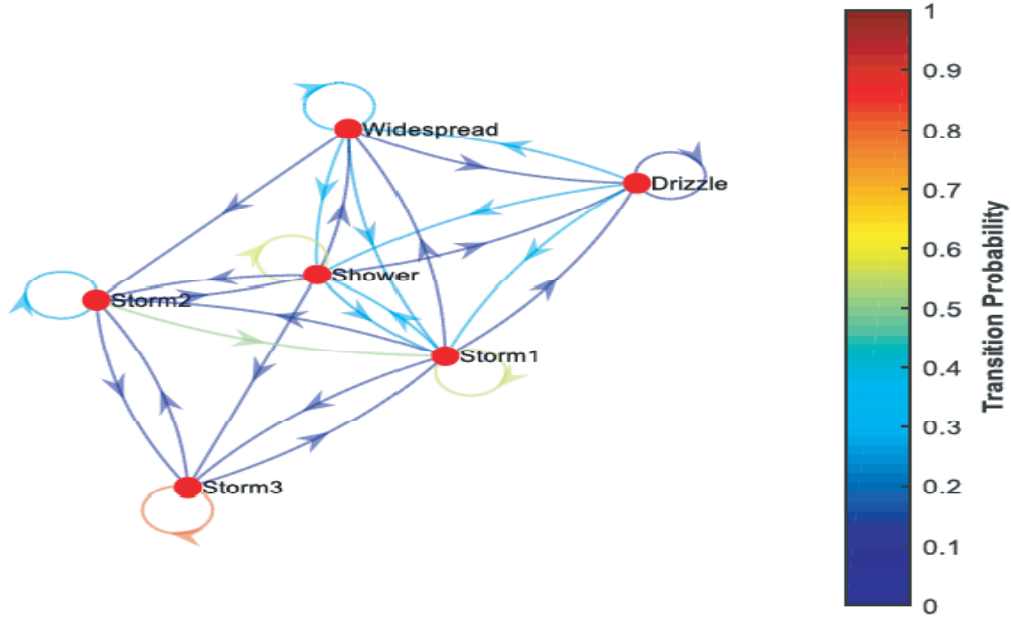
Figure 13. Spike transition graph for storm regimes.

probability matrix is a 6×6 matrix given as:

$$P_{ij,(Storms)} = \begin{bmatrix} DD & DW & DSh & DS_1 & DS_2 & DS_3 \\ WD & WW & WSh & WS_1 & WS_2 & WS_3 \\ ShD & ShW & ShSh & ShS_1 & ShS_2 & ShS_3 \\ S_1D & S_1W & S_1Sh & S_1S_1 & S_1S_2 & S_1S_3 \\ S_2D & S_2W & S_2Sh & S_2S_1 & S_2S_2 & S_2S_3 \\ S_3D & S_3W & S_3Sh & S_3S_1 & S_3S_2 & S_3S_3 \end{bmatrix} \tag{10}$$

From the measured data, the transition probability matrix in Eq. (10) is shown in the probability transition graph of Figure 13 and the spike transition probability matrix is given in Eq. (11). From the matrix in Eq. (11), it is observed that the highest transition probability occurs between two S_3 spikes with a probability of 80%.

$$P_{ij,(storms)} = \begin{bmatrix} 0.0909 & 0.2727 & 0.2727 & 0.3636 & 0 & 0 \\ 0.0714 & 0.3214 & 0.3214 & 0.2500 & 0.0357 & 0 \\ 0.0301 & 0.0902 & 0.5714 & 0.2632 & 0.0301 & 0.0150 \\ 0.0148 & 0.0370 & 0.3111 & 0.5556 & 0.0519 & 0.0296 \\ 0 & 0 & 0.1071 & 0.5000 & 0.2857 & 0.1071 \\ 0 & 0 & 0 & 0.1000 & 0.1000 & 0.8000 \end{bmatrix} \tag{11}$$

Chapman-Kolmogorov forward equations are utilized in determining the state probability k steps into a chain and are given by [5]:

$$P^{(k+1)} = \left[P^{(k)}\right] \times [P]; \quad P_{ij}^{(k+1)} = \sum_{k=0}^{n} P_{ij}^k P_{kj} \tag{12}$$

$$\Pi_j = \sum_{i=1}^{N} \Pi_i P_{ij}; \quad \sum_{j=1}^{N} \Pi_j = 1 \tag{13}$$

The final state matrices for shower regimes were deduced from Eqs. (9) and (12) as:

$$\Pi_{Sh} = \begin{bmatrix} P_D & P_W & P_{Sh} \end{bmatrix} \tag{14a}$$

$$\Pi_{Sh} = \begin{bmatrix} 0.3264 & 0.2743 & 0.3993 \end{bmatrix} \tag{14b}$$

where P_D, P_W and P_{Sh} denote the state probabilities for drizzle, widespread and shower rains. Similarly, from Eqs. (11) and (12), final state probabilities for storms regimes are as given in Eq. (15b):

$$\Pi_{St} = [\ P_D \quad P_W \quad P_{Sh} \quad P_{S_1} \quad P_{S_2} \quad P_{S_3}\ ] \tag{15a}$$

$$\Pi_{St} = [\ 0.0238 \quad 0.0769 \quad 0.3554 \quad 0.3682 \quad 0.0616 \quad 0.1142\ ] \tag{15b}$$

From Eq. (14b), it is observed that in a given shower rainfall event, shower spikes acquire the highest probability of occurrence (39.93%) as time tends to infinity, followed by drizzle spikes with a probability of 32.64%. Widespread spikes occur with the lowest probability of 27.43%. Likewise, from Eq. (15b), is observed that steady state probabilities are obtained with storm 1 spikes having the highest probability of occurrence of 36.82% followed by shower spikes at 35.54% probability occurrence. For storms, it is evident that drizzle spikes occur with the lowest probability of 2.38% followed by Storm 2 spikes with 6.16%.

A comparison of steady state Markov Chain values obtained over Durban and Jimma is shown in Table 5. Results of this comparison shows that the probability of occurrence of shower spikes is higher at both sites with values of 39.93% and 51.26% for Jimma respectively. Similarly, rain storm spikes have higher probabilities of occurrence than lower magnitude spikes at both sites with values of 36.82% and 49.90% over Durban and Jimma respectively. Further observation reveals that for rain storm regimes, drizzle spikes have the lowest probability of occurrence at both sites of observation. Contrary, for shower rainfall regimes, widespread spikes have the least probability of occurrence in Durban whereas in Jimma, drizzle spikes have the probability of occurrence. More comprehensive results are expected in future as data measurements are on-going in both Ethiopia and Butare, Rwanda.

Table 5. Markov Chain steady state values for Durban and Jimma.

Model	Regime	Markovian Steady State values			
		P_D	P_W	P_{sh}	P_{S1}
Diba et al. [10]	Shower	0.1733	0.3140	0.5126	-
(Jimma)	Storms	0.0515	0.1651	0.3344	0.4990
Durban	Shower	0.3264	0.2743	0.3993	-
	Storms	0.0238	0.0769	0.3554	0.3682

7. CONCLUSION

In this study, it is shown that the service time and its subset, the spike overlap time, follow an Erlang-k distribution, whereas the inter-arrival time follows the exponential distribution. It is also noted that there is an exponential rise in the magnitude of a storms' maximum rain rate, which clearly indicates that earth-satellite links in this region will experience higher outages than before, and it is a good premise for designers to design links and use dynamic fade mitigation techniques that are able to cope with the rise in the resultant signal attenuation. Additionally, it has been demonstrated that there is a power-law relationship between the spike's maximum rain rate and its diameter. This information is important in the determination of cell sizes and more so, in the application of site diversity technique as a fade mitigation measure. Also, this study investigates the frequency of occurrence of various magnitudes of rainfall spikes within thunderstorms rainfall regimes. The results show that rain spikes with maximum rain rates from 10 mm/h to 100 mm/h are dominant within thunderstorms in the location of study. The knowledge of the probability of occurrence of a given magnitude of a rain spike, and eventually fade magnitude and duration, is important in systems that use dynamic fade mitigation techniques.

REFERENCES

1. Foty, D., B. Smith, S. Sinha, and M. Schröter, "The wireless bandwidth crisis and the need for power-efficient bandwidth," *IEEE AFRICON Conf.*, 1–6, Livingstone, Zambia, September 2011.

2. Matricciani, E., "Prediction of fade duration due to rain in satellite communication systems," *Radio Science*, Vol. 32, No. 3, 935–941, 1997.

3. ITU-R Recommendation P. 530-16, "Propagation data and prediction methods required for the design of terrestrial line-of-sight systems," ITU, Geneva, Switzerland, 2015.

4. ITU-R Recommendation P. 530-17, "Propagation data and prediction methods required for the design of terrestrial line-of-sight systems," ITU, Geneva, Switzerland, 2017.

5. Kleinrock, L., *Queueing Systems, Vol. I, Theory*, John Wiley and Sons, New York, 1975.

6. Alonge, A. A. and T. J. Afullo, "Characteristics of rainfall queues over radio links at subtropical and equatorial Africa," *Radio Science*, Vol. 49, No. 8, 583–596, August 2014.

7. Alonge, A. A. and T. J. Afullo, "Fractal analysis of rainfall event duration for microwave and millimetric networks: Rain queueing theory," *IET Microwaves, Antennas Propag.*, Vol. 9, No. 4, 291–300, 2015.

8. Cooper, R. B., *Introduction to Queueing Theory*, 2nd Edition, Elsevier North Holland, New York, 1981.

9. Alonge, A. A. and T. J. Afullo, "Approximate queue scheduling for rainfall synthesis over radio links in subtropical regions," *IEEE Africon Proceedings*, 2015.

10. Diba, F. D., T. J. Afullo, and A. A. Alonge, "Time series rainfall spike modelling from Markov chains and queueing theory approach for rainfall attenuation over terrestrial and earth-space radio wave propagation in Jimma, Ethiopia," *2016 Progress In Electromagnetic Research Symposium (PIERS)*, 4991–4995, Shanghai, China, Aug. 8–11, 2016.

11. Begum, S. and I. E. Otung, "Rain cell size distribution inferred from rain gauge and radar data in the UK," *Radio Sci.*, Vol. 44, RS2015, 2009, doi:10.1029/2008RS003984.

12. Akuon, P. O. and T. J. O. Afullo, "Rain cell sizing for the design of high capacity radio link systems in South Africa," *Progress In Electromagnetics Research B*, Vol. 35, 263–285, 2011.

13. Rambaugh, J., I. Jacobson, and G. Booch, *The Unified Modelling Language Reference Manual*, 2nd Edition, Pearson, Boston, 2005.

14. Ahuna, M. N., T. J. Afullo, and A. A. Alonge, "30-second and one-minute rainfall rate modelling and conversion for millimetric wave propagation in South Africa," *SAIEE ARJ*, Vol. 107, No. 1, 17–29, March 2016.

15. Ahuna, M. N., T. J. Afullo, and A. A. Alonge, "Rainfall rate prediction based on artificial neural networks for rain fade mitigation over earth-satellite link," *IEEE Africon Proceedings*, 579–584, September 2017.

16. Adan, I. and J. Resing, *Queueing Systems*, Netherlands, 2015.

17. Akuon, P. O. and T. J. O. Afullo, "Rain cell size statistics from rain gauge data for site diversity planning and attenuation prediction," *SATNAC Proceedings*, September 4–7, 2011.

18. Pawlina, A., "No rain intervals within rain events: Some statistics based on Milano radar and rain-gauge data," *COST Action 280, 1st International Workshop*, July 2002.

19. Bolch, G., S. Greiner, H. de Meer, and K. S. Trivedi, *Queueing Networks and Markov Chains*, John Wiley and Sons, New York, 1998.